scientific reports

Check for updates

OPEN

CDX1 improves nicotine induced cardiac fibroblasts activation and cardiomyocyte hypertrophy by alleviating autophagic flux impairment through modulation of LAPTM4B

Yue-yan Li[1,2], Fan-liang Meng[3], Si-yuan Zhou[1], Jia-min Du[1], Wen-jing Li[2], Qi-yun Liu[4], Lei Wu[2], Meng-meng Zhao[2], Yi Jin[2], Qun-ye Zhang[5], Ying Li[1,2]✉ & Guo-hai Su[1,2]✉

Nicotine-induced impairment of autophagic flux promotes the onset of myocardial remodelling, thereby exacerbating heart failure. In this study, we investigated the role and molecular mechanisms of the transcription factor CDX1 in cardiac fibroblasts (CFs) activation and cardiomyocyte hypertrophy induced by nicotine. We found that CDX1 expression was increased in response to nicotine. However, a decrease in CDX1 further exacerbated the nicotine-induced blockade of autophagic flux, thereby aggravating CFs activation and cardiomyocyte hypertrophy. This effect was attributed to the suppression of the autophagic regulator LAPTM4B transcription by CDX1 and the subsequent activation of the mTOR pathway. In contrast, CDX1 overexpression promoted LAPTM4B expression, resulting in the opposite effect. In conclusion, our study demonstrated that CDX1/LAPTM4B axis could alleviate nicotine-induced autophagy flux impairment by inhibiting mTORC1 pathway activation, thereby alleviating CFs activation and cardiomyocyte hypertrophy, and exerting cardioprotective functions.

Keywords CDX1, LAPTM4B, Autophagic flux, Nicotine, Cardiomyocyte hypertrophy, Fibroblast activation

Heart failure (HF) is a condition of reduced cardiac output caused by various structural or functional diseases of the heart and is associated with a high mortality rate. Although some progress has been made in the treatment of heart failure in clinical practice, the prognosis of heart failure remains unsatisfactory[1]. Myocardial remodeling is the initiating factor in the development of heart failure, and the central events in this process arise from cardiomyocyte hypertrophy and cardiac fibroblast activation[2]. Numerous studies have shown that abnormal regulation of autophagy is involved in the pathological process of myocardial remodeling[3–5]. Macroautophagy (known as autophagy) is a highly conserved metabolic process in eukaryotic organisms that maintains the cycling and renewal of cellular nutrients in organisms through the selective degradation of proteins and the damaged organelles. Autophagic flux refers to the dynamic processes of autophagy within cells, encompassing the formation, fusion, degradation, and recycling of autophagosomes. Autophagy is a critical cellular mechanism that enables cells to eliminate damaged organelles, aggregated proteins, and various metabolic byproducts, thus maintaining cellular homeostasis and function. Specifically, in autophagy, vesicles with bilateral membrane structures engulf functionally impaired organelles or proteins to form early autophagic vesicles, which finally bind to lysosomes to form late autophagic lysosomes, which degrade and remove harmful substances while recycling them[6,7]. Similarly, activation of autophagy plays an important role in protecting the heart from nicotine

[1]Department of Cardiology, Jinan Central Hospital, Shandong University, Jinan, China. [2]Research Center for Translational Medicine, Central Hospital Affiliated to Shandong First Medical University, Jinan, China. [3]Affiliated Hospital of Shandong University of Traditional Chinese Medicine, Jinan, China. [4]Department of Cardiology, Shandong Second Medical University, Weifang, China. [5]The Key Laboratory of Cardiovascular Remodeling and Function Research, Department of Cardiology, Qilu Hospital, Shandong University, Jinan 250012, China. ✉email: liying0766@email.sdu.edu.cn; gttstg@163.com

damage. Studies have shown that inhibition of normal autophagy levels can lead to the development of cardiac hypertrophy, which can be attenuated by restoring normal autophagy levels[8–11]. However, the specific molecular mechanism of autophagy regulation in this process remains unclear.

Smoking is an independent risk factor for cardiovascular disease. Nicotine, one of the main harmful substances in tobacco, has been shown to play an important role in the development of cardiac remodeling[12,13]. Autophagic flux blockade and myocardial hypertrophy occur in cardiomyocytes under the stimulation of nicotine[13]. Alleviation of autophagic flux impairment can inhibit myocardial remodeling and protect cardiac function[14,15]. This is consistent with our previous study[16]. However, other mechanisms of autophagy regulation involved in nicotine-induced myocardial remodeling remain to be elucidated. In the present study, we found that Caudal related homeobox 1 (CDX1) was responsively up-regulated in response to nicotine stimulation, but its role in nicotine-induced myocardial injury has not been reported.

CDX1 is a member of the CDX family[17] and previous research focused on gastrointestinal tumors. CDX1 is also a crucial transcription factor in the initial stages of heart development in the mammalian embryos[18] and it plays a role in regulating epicardial cell differentiation through the PI3K/AKT signaling pathway[19]. However, little is known about its function in the heart. Recently, CDX1 was found to promote proliferation and resist apoptosis in colon cancer stem cells by initiating autophagy, whereas its absence leads to a reduction in autophagic flux in these cells[20]. However, it is largely unknown whether CDX1 influences the process of nicotine-induced myocardial injury by regulating autophagy. Cardiomyocyte injury is closely associated with lysosomal dysfunction and impaired clearance of autophagic vesicles[21]. Defects in lysosomal membrane proteins can lead to the accumulation of autophagosomes and the autophagic substrate. The role of lysosomal membrane proteins in nicotine-induced impairment of autophagic flux in cardiomyocytes is not fully understood. Lysosome-associated transmembrane protein 4B (LAPTM4B), which was predicted to be a downstream target gene of the CDX1 transcription factor, plays a crucial role in modulating autophagic flux.

LAPTM4B, a member of the lysosomal transmembrane protein family, localizes to lysosomes and stabilizes lysosomal membranes[22], and is highly expressed in cardiac muscle[23]. Down-regulation of LAPTM4B has been shown to prevent lysosomes from binding to autophagosomes to form autophagic lysosomes at the late stage of autophagy in starved breast cancer cells, thereby blocking autophagic flux[24]. LAPTM4B interacts with EGFR to initiate autophagy and promote tumour cell survival[25]. Overexpression of LAPTM4B can alleviate the autophagic flux impairment induced by myocardial ischemia/reperfusion in mice through the AKT/mTOR pathway and play a role in protecting cardiac function[26]. Recently, nicotine has been shown to stimulate the upregulation of LAPTM4B[27]. In lung cancer patients, LAPTM4B expression was significantly higher in smokers than in non-smokers[28]. Therefore, we speculated that CDX1 may play a cardioprotective role during nicotine-induced myocardial remodelling by targeting and regulating LAPTM4B to participate in the autophagy process.

The mammalian target of rapamycin complex 1 (mTORC1) plays an important regulatory role in autophagy and is a key negative regulator of autophagy[29,30]. mTORC1 inhibits catabolic processes, including autophagy[27,31]. Inhibition of the mTORC1 pathway by pharmacological or genetic means increases autophagy in cardiomyocytes[30,32–34]. Lysosomal membrane proteins are important targets for mTOR, but whether CDX1/LAPTM4B acts through this pathway remains unclear.

The aim of this study was to investigate the role and potential molecular mechanism of CDX1 in nicotine-induced cardiomyocyte hypertrophy and activation of CFs by modulation of autophagy. The results of this study may provide potential new targets for myocardial remodeling and the prevention and treatment of heart failure.

Materials and methods

Reagents

Nicotine and BafA1 were purchased from Sigma-Aldrich. Type II collagen was purchased from Worthington Biochemical Company, USA. Taq Pro Universal SYBR qPCR Master Mix and Trizol Reagent were purchased from Hunan Accurate biology, HUNAN China. Protein molecular weight standards and lipo®2000 were purchased from Thermo Fisher, USA. Opti-MEM medium and fetal bovine serum were purchased from GIBCO, USA. Specific NC siRNA(5'-UUCUCCGAACGUGUCACGUTT-3'; 3'-ACGUGACACGUUCGGAGAATT-5'), specific LAPTM4B siRNA (siRNA1: 5'-TGTCATCCTTCTCTTCATA-3') and specific CDX1 siRNA (siRNA: 5'-CGACTGGGCAGCTGCCTAT-3') were purchased from RIBOBIO (Guangzhou, China). Primers used for q-PCR and Antibodies are shown in key resources Tables 1 and 2.

Methods

Extraction of NRVMs and cardiac fibroblasts(CFs)

The CFs[35] and NRVMs[36] were prepared in accordance with the previously described methodology. In brief, 1- to 3-day-old Wistar rats were anesthetized with 2% isoflurane, followed by euthanasia through cervical dislocation. After euthanasia, the skin of the pups was promptly disinfected, an incision was made, and the heart was carefully extracted. The ventricular tissues were then digested with phosphate-buffered saline (PBS) containing 200 U type II collagenase and 0.4% horse serum for three cycles. Subsequently, the cells were suspended and centrifuged in medium containing 5% fetal bovine serum and 8% horse serum. The cell suspensions were incubated at 37°C with 95% O_2 and 5% CO_2 for 1.5 h. The NRVMs were suspended in the culture medium, while the CFs were adhered to the wall of the culture flasks. The suspended NRVMs were removed and plated in 1×10^5 cells/ml of culture medium. Additionally, 0.1 mM 5-bromo-2-deoxyuridine (BrdU) was added to the medium to inhibit non-NRVMs. Prior to the experiment, the cells were cultured in serum-free medium for 24 h. The majority of cells (>95%) were identified as NRVMs based on morphological examination and anti-actin antibody staining. With regard to the previously adherent CFs, cell suspensions were prepared after two days by digestion with 0.25% trypsin, cultured in medium containing 4% fetal bovine serum and passaged at a 1:4 ratio. In subsequent experiments, third-generation cells were employed. All media were supplemented with 1%

Primers used for q-PCR	
Genes	**Sequences (5'-3')**
β-actin	5'-CGTTGACATCCGTAAAGACC-3' (forward)
	5'-TAGAGCCACCAATCCACACA-3 '(reverse)
BNP	5'-GCTGCTTTGGGCAGAAGATA-3'(forward)
	5'-GGAGTCTGCAGCCAGGAGGT-3 '(reverse)
ANP	5'-GGGGGTAGGATTGACAGGAT-3'(forward)
	5'-GGGATCTTTTGCGATCTGCTC-3 '(reverse)
β-MHC	5'-CGCTCAGTCATGGCGGAT-3'(forward)
	5'-GCCCCAAATGCAGCCAT-3 '(reverse)
Col1	5'-CCAGCGGTGGTTATGACTTCA-3'(forward)
	5'-TGCTGGCTCAGGCTCTTGA-3 '(reverse)
Col3	5-GGTCACTTTCACTGGTTGACGA-3'(forward)
	5'-TTGAATATCAAACACGCAAGGC-3 ' (reverse)
a-SMA	5'-CATCCGACCTTGCTAACGGA-3' (forward)
	5'-GTCCAGAGCGACATAGCACA-3 ' (reverse)
Fn	5'-GGATCCCCTCCCAGAGAAGT-3' (forward)
	5'-GGGTGTGTGGAAGGGTAACCAG-3 ' (reverse)
CDX1	5'-AGCAGCAGCAGCAGCAACAG – 3' (forward)
	5'-CAGCATTGGTGGGGCATAGACTC – 3 ' (reverse)
LAPTM4B	5'-CCTGATCATCAATGCCGTGG-3'(forward)
	5'-CATGAGGAGAGAGATCGCGA- 3' (reverse)

Table 1. The reverse primer sequences and forward primer sequence of the target gene used for q-PCR.

Antibodies			
Target antigen	**Vendor or source**	**Catalog #**	**Working concentration**
phosphor-4EBP1	Cell signaling technology	2855s	1:1000 WB
phosphor-p70s6k	Cell signaling technology	9204s	1:1000 WB
p70s6k	Cell signaling technology	2708s	1:1000 WB
phosphor-mTOR	Cell signaling technology	5536s	1:1000 WB
α-SMA	ABclonal	A1011	1:1000 WB
LAPTM4B	abcam	ab25631	1:1000 WB
4EBP1	Proteintech	60246-1-Ig	1:1000 WB
mTOR	Proteintech	66888-1-Ig	1:1000 WB
p62	Proteintech	14600-1-AP	1:1000 WB
,LC3II	Proteintech	66184-1-Ig	1:1000 WB
β-actin	Proteintech	66009-1-Ig	1:2000 WB
Col1	Proteintech	66761-1-Ig	1:1000 WB
Col3	Proteintech	22734-1-AP	1:1000 WB
GAPDH	Proteintech	60004-1-Ig	1:2000 WB
CDX1	Sigma-Aldrich	PM045	1:100 WB

Table 2. The sources, catalog numbers, and working concentrations of all antibodies used in this study are listed.

streptomycin-penicillin. All methods were carried out in accordance with relevant guidelines and regulations and are reported in accordance with ARRIVE guidelines. The experimental procedures carried out in the present study were approved by the Animal Ethics Committee.

Method details

Adenoviral transfection and SiRNA transfection of cells

To obtain stable CDX1 and LAPTM4B overexpressing cells and corresponding negative control cells, we infected NRVMs and CFs with negative control(NC 1:3000 dilution), adenovirus-mediated LAPTM4B overexpression AdLAPTM4B 1:5000 dilution, NO.CON176) and adenovirus-mediated CDX1 overexpression (AdCDX1 1:3000 dilution, NO. CON174) constructed by Genechem (Shanghai, China). After 8 h of incubation, the medium was replaced with normal medium, and PCR and WB were performed to detect transfection efficiency after 24 and 48 h, respectively. NRVMs and CFs were transfected with recombinant adenovirus encoding mCherry-

EGFP-LC3 (2×10^{10} PFU/ml stock solution, 1:5000 dilution) (HANBIO, Wuhan, China), and experiments were performed after 48 h of incubation.

Knockdown of CDX1 and LAPTM4B was performed by using siRNA. NRVMs and CFs were inoculated into 6-well plates at 1×10^5 cells per well. Cells were transfected with siLAPTM4B and siCDX1 in Opti-MEM medium with Lipo® 2000 reagent; negative controls were transfected scrambled RNA (si-NC). After 6 h, the medium was changed to normal medium, and cells were continuously cultured for 24 h for PCR and WB assays.

Western blot

Immunoblotting and quantification of relative protein levels were performed as described in a previous study[37]. The cells were lysed with protein lysate. The protein concentration of the homogenates was determined and quantified using the Kaumas Brilliant Blue protein assay. Protein extracts were electrophoresed in SDS-PAGE gels and then transferred to PVDF membranes. Anti-p62, anti-LC3, anti-Col1, anti-Col3, anti-α-SMA, anti-LAPTM4B, anti-p-p70s6k, anti-p70s6k, anti-p-4EBP1, anti-4EBP1, anti-p-mTOR, anti-mTOR, anti-CDX1, anti-GAPDH, and anti-β-ACTIN were added, and the above proteins were detected with horseradish peroxidase-coupled IgG secondary antibodies (1:2000 dilution) to detect the above proteins. The immunoblotting signals of the protein bands were visualized using the Tanon imaging system. The bands were analyzed in greyscale using Image J software (version 1.46r, Wayne Rathband, National Institutes of Health, USA) and normalized to the level of β-actin or GAPDH.

Dual luciferase reporter gene test

293T cells were inoculated and cultured in 24-well plates. Cells were co-transfected with LAPTM4B promoter luciferase plasmid and CDX1 adenoviral vector (Promega, Madison, WI, USA) after 24 h and replaced with normal medium after 8 h. After 48 h, luciferase activity was analyzed using the Dual Luciferase Reporter Assay System (Promega). The values of luciferase activity of each group were normalized to the level of sea pansy luciferase.

Quantitative reverse transcription polymerase chain reaction (qRT-PCR)

Total RNA was extracted from NRVMs and CFs using Trizol, and cDNA was synthesized by reverse transcription using the method described previously[36]. cDNA was synthesized by applying fluorescence quantitative polymerase chain reaction using the ABI7500 system. The following primers were used in this study β-actin, BNP, ANP, β-MHC, Col1, Col3, α-SMA, Fn, CDX1, LAPTM4B, and the primer sequences are shown in Table 1. All the above primers were denatured at 95 °C (30 s) each, and PCR was performed with 40 cycles of annealing set (95 °C (5 s), 60 °C (30 s)) reaction, and the mRNA level of each target gene was normalized to the β-actin level.

Immunofluorescence

The culture medium was removed, and cells were washed three times with PBS, fixed with 4% paraformaldehyde for 20 min, washed with PBS and then permeabilized with 0.3% Triton X-100 for 3 min. After blocking with 10% donkey serum for 40 min, cells were incubated overnight at 4 °C with primary antibodies (1:200 dilution) against α-SMA. Following three PBS washes, cells were incubated.Nuclei were stained.

Collagen gel contraction (CGC) assay

The collagen gel contraction (CGC) assay was used to assess the contraction ability of CFs under nicotine stimulation. After being trypsinized, CFs were suspended in medium and mixed with collagen gel working solution (CBA-201, Cell Biolabs, San Diego, CA) on ice. The collagen mixture (1×10^5 cells/mL) was then seeded in a 24-well plate. After incubating at 37 °C for 1 h, the collagen gel was allowed to solidify. The edges of the gel were separated from the well walls, and medium containing nicotine was added to the gel. Control groups were treated with medium without nicotine. The cell contractility was measured 12–24 h later. Finally, gel images were captured and analyzed using ImageJ software.

Hematoxylin-eosin staining (HE staining)

HE staining was used to evaluate cardiomyocyte area. After culturing, cells were treated with nicotine or vehicle for 48 h, fixed with 4% paraformaldehyde for 10 min, and washed with PBS three times. Following fixation, cells were stained with hematoxylin and eosin, dehydrated with graded ethanol, vitrified in xylene, and mounted with neutral gum. Microscopic images were captured for analysis.

Statistical analysis

An unpaired t-test were employed to statistically assess the differences between the two groups. Comparisons of differences between more than three groups were analyzed using one-way analysis of variance (ANOVA), Bonferroni test employed for post-hoc analyses. Comparative tests between multiple groups were applied using GraphPad Prism software (version 8.0.3, California, USA). The data were processed using Adobe Photoshop CS 6 software (version 13.0, California, USA). The mean value was derived from at least three independent biological experiments, with each experiment performed in triplicate to ensure stable and reliable results.The normality of the data was assessed using the Shapiro-Wilk test, and the homogeneity of variances was evaluated with Brown-Forsythe test. The data in this study were tested for normality and found to satisfy the assumption of homogeneity of variance. Detailed data are provided in the supplementary explanatory document. The data are expressed as mean ± standard deviation. P values less than 0.05 were considered statistically significant differences.

Results

Nicotine induces cardiomyocyte hypertrophy and activation of CFs by impairing autophagic flux

To confirm the effect of nicotine on CFs, we applied nicotine (0.1 nM, 10 nM, 100 nM, 500 nM) to stimulate CFs for 48 h. As shown in Fig. 1A, the mRNA levels of myocardial fibrosis markers Col1, Col3, α-SMA and FN

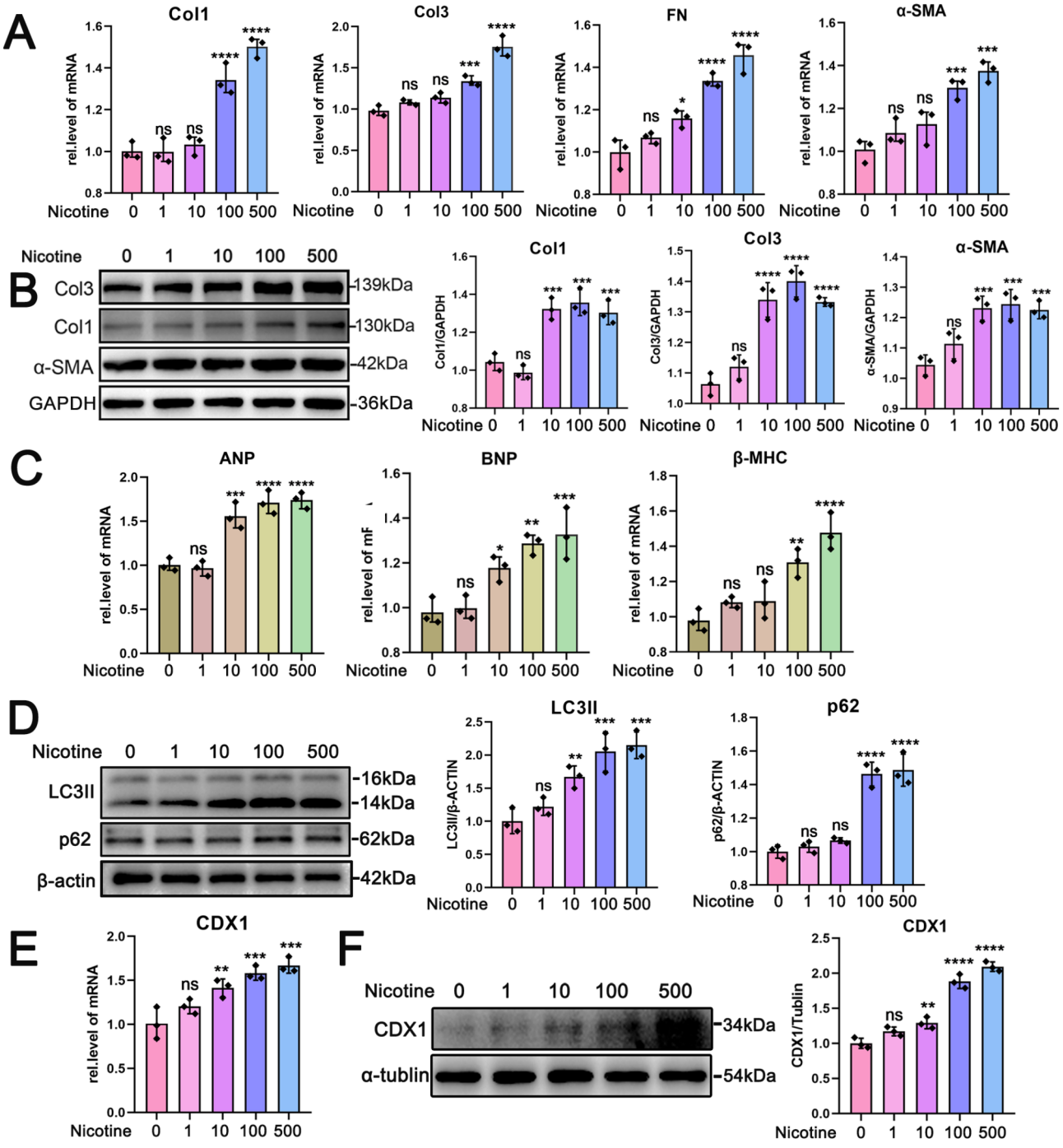

Fig. 1. Nicotine causes activation of CFs and hypertrophy of NRVMs by inducing autophagic flux blockade. The mRNA expression of myocardial fibrosis markers Col1, Col3, α-SMA, FN (**A**) and myocardial hypertrophy markers ANP, BNP, β-MHC (**C**) were detected by qPCR. The protein expression of myocardial fibrosis markers was detected by Western blot (WB) (**B**). Expression of autophagy marker LC3II and its specific substrate p62 in nicotine-stimulated CFs was detected by WB (**D**). The mRNA level of CDX1 was detected by qPCR in CFs stimulated with different concentrations of nicotine (**E**), and the protein expression level of CDX1 was detected by WB (**F**). Results are given as mean ± SD, P value was determined by one-way AVONA with Bonferroni test, **** $p < 0.0001$; *** $p < 0.001$; ** $p < 0.01$; * $p < 0.05$, $n = 3$.

were significantly increased in a concentration-dependent manner as detected by PCR under the stimulation of nicotine. Elevated α-SMA is a marker of cardiac fibroblast activation. Meanwhile, Col1, Col3 and α-SMA were examined at the protein level and the results showed the existence of similar trends (Fig. 1B). Similarly, after applying exposure doses of nicotine (0.1 μM, 10 μM, 100 μM, 500 μM) to stimulate NRVMs for 48 h, the mRNA levels of cardiac hypertrophy markers ANP, BNP and β-MHC were significantly increased as detected by applying qRT-PCR (Fig. 1C). CFs exhibited a clear tendency to differentiate into α-SMA-positive myofibroblasts under nicotine stimulation(Figure S1A). The collagen gel contraction assay confirmed that CFs exhibited a significant increase in contractile ability under nicotine treatment.(FigureS1B). As shown in Supplementary Fig. 1 C, the cardiomyocytes surface area were significantly increased after treatment with nicotine. The results indicated that nicotine induced the activation of CFs and the development of cardiomyocyte hypertrophy. It has been confirmed[16]. LC3II, an insoluble autophagosome-associated form, often represents the activation of autophagy, and p62 is a selective substrate for autophagy. In the present study, LC3II was significantly increased in CFs under nicotine stimulation (Fig. 1D). To distinguish whether the increase in LC3II was due to activation of autophagy or impairment of autophagic flux, we examined the levels of the autophagic substrate p62 and showed that p62 also showed significant accumulation (Fig. 1D). In NRVMs, both LC3II and p62 showed nicotine concentration-dependent accumulation (Figure S1D). Thus, in CFs and NRVMs, nicotine may contribute to the developmental process of CFs activation and myocardial cell hypertrophy by impairing autophagic flux.

Under nicotine stimulation, both mRNA and protein levels of CDX1 appeared to be concentration-dependently increased in CFs (Fig. 1E and F), and showed the same changes in NRVMs (Figure S1E,1 F). These findings indicate that CDX1 is potentially involved in mediating nicotine-induced damage to cardiomyocytes.

CDX1 is a critical regulator of nicotine-induced activation of CFs and cardiomyocyte hypertrophy

To further clarify the biological function of CDX1 in CFs and NRVMs, we applied CDX1 siRNA and its negative control to transfect CFs, which resulted in a significant downregulation of CDX1 mRNA levels in cells compared with the control(Figure S1G), and the same effect was shared in NRVMs(Figure S1I). CFs were stimulated with 500 nM nicotine, while NRVMs were treated with 100μM nicotine. To our surprise, after knockdown of CDX1, the mRNA levels of Col1, Col3, α-SMA and FN appeared to be more significantly upregulated in response to nicotine. Notably, the reduction in CDX1 expression alone also showed a slight upregulation compared to controls and was statistically significant (Fig. 2A). Subsequently, the protein levels of Col1, Col3, α-SMA showed the same changes (Fig. 2B). Similarly, the mRNA levels of ANP, BNP and β-MHC all showed a more significant increase after CDX1 downregulation in nicotine-exposed NRVMs (Fig. 2C).We then used adenovirus-mediated CDX1 overexpression (AdCDX1) and negative control vector (NC) to transfect CFs and NRVMs, which resulted in a significant upregulation of CDX1 mRNA levels in the cells (Figure S1H, Figure S1J). CDX1 overexpression reduced the gene levels of Col1, Col3, α-SMA and FN in nicotine + Ad-CDX1 groupcompared to the nicotine group (Fig. 2D), which was similarly confirmed by protein level assays of Col1, Col3, α-SMA (Fig. 2E). In NRVMs, it was observed that the overexpression of CDX1 significantly inhibited the upregulation of ANP, BNP, and β-MHC induced by nicotine (Fig. 2F). The above data suggest that nicotine-stimulated downregulation of CDX1 expression further promotes CF activation and cardiomyocyte hypertrophy. However, the overexpression of CDX1 partially reversed the nicotine-induced activation of CFs and cardiomyocyte hypertrophy. Therefore, the increase in CDX1 expression in response to nicotine stimulation appears to initiate a protective mechanism.

CDX1 improves nicotine-induced activation of CFs and cardiomyocyte hypertrophy by alleviating autophagic flux impairment

Nicotine has been shown to impair autophagic flux, leading to activation of CFs and hypertrophy of NRVMs[16]. However, whether CDX1 involves in this process is unknown. CDX1 has been shown to be involved in the regulation of autophagy. Therefore, we speculated that CDX1 may be involved in the regulation of activation of CFs and cardiomyocyte hypertrophy by modulating autophagy. As shown in Fig. 3A, after downregulation of CDX1 expression in CFs in response to nicotine, the protein level of LC3II was significantly increased compared to the nicotine group. Similarly, p62 expression was significantly accumulated in the nicotine-stimulated siCDX1 group. At the same time, we observed that LC3II and p62 were also significantly increased after CDX1 downregulation alone compared to the control group. This phenomenon was similar in NRVMs, suggesting that autophagic flux may be impaired after downregulation of CDX1(Figure S2A). In contrast, after CDX1 overexpression, LC3II was increased in cells compared to controls and further increased in response to nicotine. In contrast to LC3II, nicotine-induced p62 accumulation after AdCDX1 was significantly attenuated compared to the nicotine group (Fig. 3B). We observed the same trend in NRVMs (Figure S2B).

To further assess the effect of CDX1 on autophagosome accumulation and autophagolysosome formation, we differentiated between early autophagosomes and acidified autophagolysosomes by transfecting CFs and NRVMs with adenoviral-mediated mCherry-EGFP tandem-tagged with LC3, which is readily degraded in the acidic environment of autophagosomes fused with lysosomes and quenched by green light. Therefore, autophagy normally proceeds with the process being detected mainly by red light particles. When the autophagic process is blocked, cells express both red and green light and show yellow fluorescent particles, representing the lack of autophagic lysosomes and the accumulation of autophagosomes. We used BafA1 and rapamycin (Rapa), a commonly used autophagy activator that inhibits mTOR, respectively, as controls. In CFs, CDX1 overexpression led to a significant increase in red light particles, which was similar to what was observed in the rapamycin group. In contrast, down-regulation of CDX1 resulted in a significant increase in yellow light particles, indicating an accumulation of autophagic vesicles and a blockage of the autophagic flux. Under nicotine stimulation, the upregulation of CDX1 led to a decrease in yellow fluorescent particles and an increase in red fluorescent particles, thereby inhibiting nicotine-induced accumulation of autophagic vesicles and blockage of autophagic

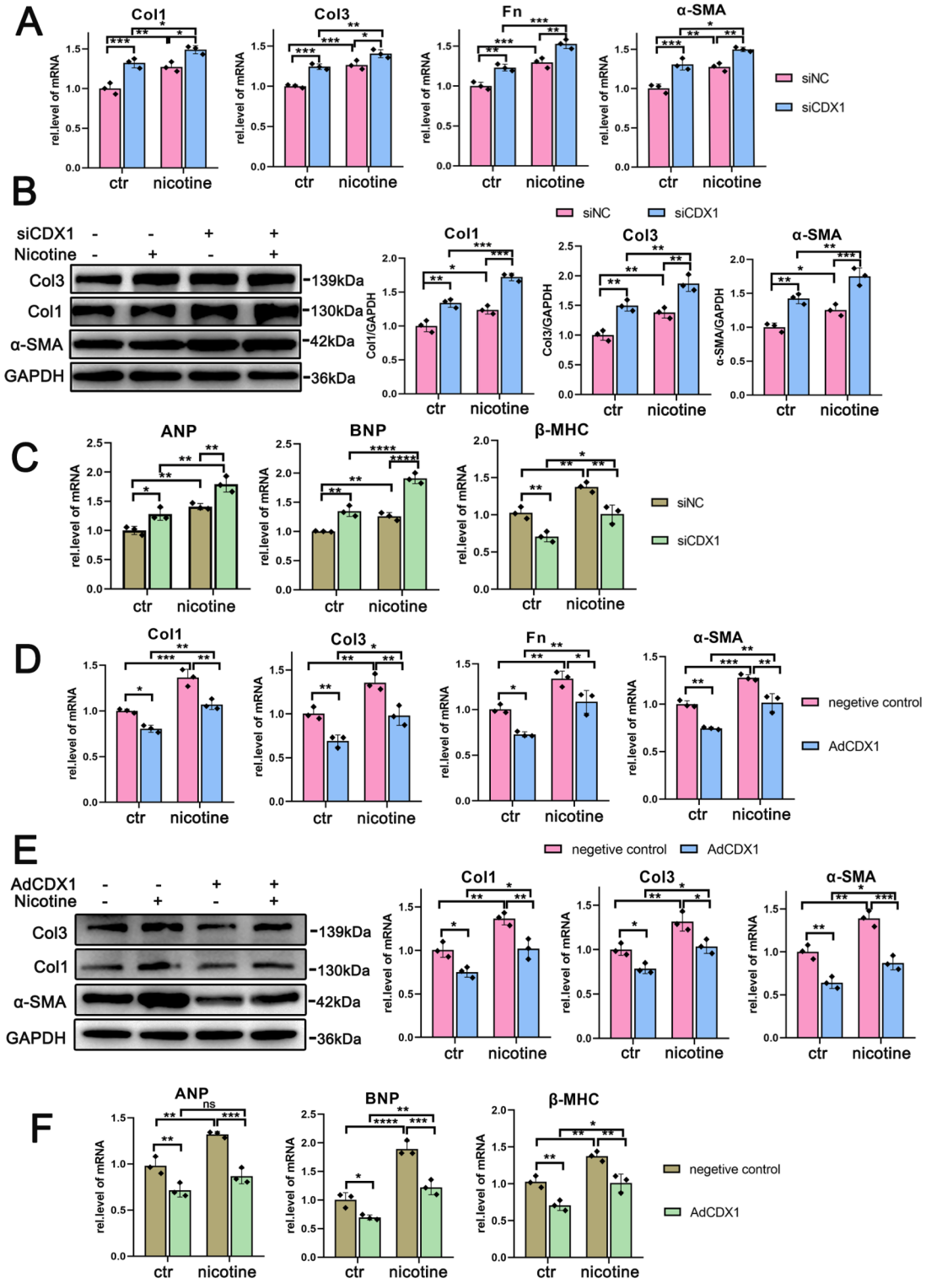

Fig. 2. CDX1 is upregulated in response to nicotine, and downregulation of CDX1 exacerbates nicotine-induced activation of CFs and cardiomyocyte hypertrophy. The mRNA expression of cardiac fibrosis markers Col1, Col3, α-SMA, FN in CFs with CDX1 knockdown (siCDX1) (**A**) and cardiac hypertrophy markers ANP, BNP, β-MHC in NRVMs (**C**) were detected by applying qPCR. The protein expression of Col1, Col3, α-SMA, FN upon downregulation of CDX1 was detected by WB (**B**). The mRNA expression of Col1, Col3, α-SMA, FN in CFs during CDX1 overexpression (AdCDX1) (**D**) and the mRNA expression of ANP, BNP, β-MHC in NRVMs were detected by qPCR (**F**). WB was used to detect the protein expression of Col1, Col3, α-SMA, FN in AdCDX1 (**E**). Results are given as mean ± SD, P value was determined by two-way AVONA with Bonferroni test, **** $p < 0.0001$; *** $p < 0.001$; ** $p < 0.01$; * $p < 0.05$, $n = 3$.

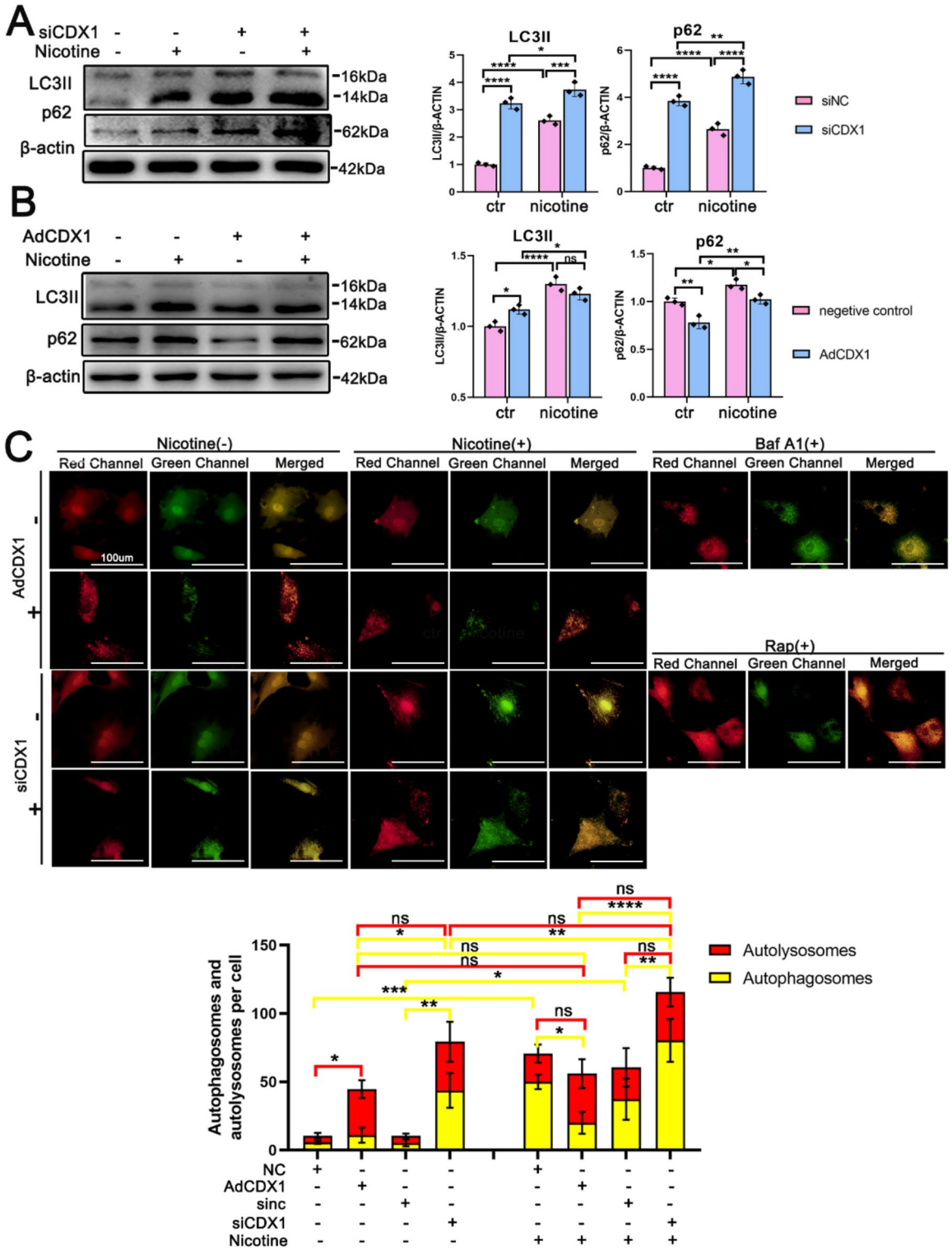

Fig. 3. CDX1 exacerbates nicotine-induced CFs activation and cardiomyocyte hypertrophy by inducing autophagic flux blockade . Expression of autophagy markers LC3II and p62 after CDX1 downregulation (siCDX1) was detected in CFs by WB (**A**), and expression of LC3II and p62 after CDX1 overexpression (AdCDX1) was similarly detected (**B**). Results are given as mean ± SD, P value was determined by two-way AVONA with Bonferroni test, **** $p < 0.0001$; *** $p < 0.001$; ** $p < 0.01$; * $p < 0.05$, $n = 3$. Representative images of autophagosomes (yellow dots) and autolysosomes (red dots) in each cell after CDX1 overexpression (AdCDX1) or knockdown (siCDX1) in the presence or absence of nicotine stimulation conditions, using Baf A1 (100 nM) and Rapa (10μM) as control, and mCherry-EGFP-LC3 transfected CFs (**C**). Representative of $n = 3$ experiments, scale bar = 100 μm.

flux. Conversely, the knockdown of CDX1 showed the opposite tendency, further exacerbating the accumulation of autophagic vesicles, similar to the results observed in the Baf A1group (Fig. 3C). These findings were also observed in NRVMs (Figure S2C).

We next investigated whether CDX1 protects cardiomyocytes by alleviating nicotine-stimulated autophagic flux impairment. In CFs and NRVMs overexpressing CDX1, we applied Baf A1 to block autophagic flux. BafA1 acts as an inhibitor of late autophagy by preventing the fusion of autophagic vesicles with autophagic lysosomes. Our results showed that Baf A1 treatment resulted in a significant accumulation of LC3II and p62 in both the control and nicotine groups. Moreover, it abolished the protective effect of CDX1 overexpression on p62 accumulation in the presence of nicotine (Fig. 4A, Figure S3A). Furthermore, rapamycin exhibited a slight increase in LC3II levels in control cells, while a slight decrease was observed in cells with siCDX1(Fig. 4B). The elevated levels of LC3II and p62 proteins were significantly diminished in CFs in which rapa had downregulated CDX1 in response to nicotine stimulation (Fig. 4B). The same changes were observed in NRVMs (Figure S3B). The above results suggest that CDX1 plays a key role in nicotine-induced autophagic flux injury.

Additionally, we observed that protective effects conferred by CDX1 overexpression in the activation of CFs and hypertrophy of NRVMs were negated by BafA1 stimulation, as evidenced by the evaluation of the expression levels of Col1, Col3, α-SMA, and FN, as well as ANP, BNP, and β-MHC (Fig. 4C and D). Therefore, the reduction in CDX1 expression in response to nicotine resulted in further impairment of autophagic flux, thereby exacerbating the damage caused by nicotine. Conversely, as shown in Fig. S3C, downregulation of CDX1 expression exacerbates the nicotine-induced increase in Col1, Col3, α-SMA, and FN. However, this effect induced by nicotine alone or in combination with CDX1 downregulation was alleviated under the influence of the autophagy activator rapamycin. We observed a similar phenomenon in NRVMs, where the elevated levels of ANP, BNP, and β-MHC induced by nicotine alone or in combination with siCDX1 were reduced under the influence of rapamycin (Fig. S3D). Consequently, the elevation of CDX1 levels during nicotine exposure may serve as an optimization mechanism of cardiac development, potentially alleviating the blockade of autophagic flux.

LAPTM4B is a downstream target gene of CDX1 and is positively regulated by CDX1

According to the target gene-promoter prediction website, CDX1 is predicted to be a potential transcription factor of the LAPTM4B promoter. This finding suggests a potential regulatory relationship between CDX1 and LAPTM4B. Notably, LAPTM4B has been implicated in smoking-related processes and the regulation of autophagy. To further clarify the relationship between CDX1 and LAPTM4B, a dual luciferase reporter gene assay was conducted. The results, as shown in Fig. 5A, showed that the CDX1 transcription factor promoted the transcription of LAPTM4B, suggesting that CDX1 functions as an upstream transcription factor of LAPTM4B. As shown, there was a concentration-dependent upregulation of the protein level of LAPTM4B in CFs (Fig. 5B) and NRVMs (Figure S3E) in response to nicotine. Subsequent analysis of mRNA levels revealed a consistent pattern (Fig. 5C, Figure S3F). To further elucidate the relationship between CDX1 transcription factors and LAPTM4B, we examined the expression levels of LAPTM4B following up- or down-regulation of CDX1. The results demonstrated that the RNA level (Fig. 5D) and the protein level (Fig. 5E and F) of LAPTM4B were significantly elevated in CFs after CDX1 up-regulation. The down-regulation of CDX1 had the opposite result. Similarly, the same changes were also found at the protein(Figure S4A, 4B)and gene(Figure S4C, 4D) levels in NRVMs, indicating a positive regulatory relationship on the expression of LAPTM4B by CDX1.

The downregulation of LAPTM4B exacerbates the blockade of autophagic flux induced by nicotine, thereby accelerating the progression of activation of CFs and hypertrophy of cardiomyocytes

To further investigate the role of LAPTM4B in the heart, adenovirus-mediated overexpression of LAPTM4B and small interfering RNA-mediated down-regulation of LAPTM4B were utilized to transfect CFs (Figure S4E) and NRVMs (Figure S4F).Given that LAPTM4B is localized in the lysosomal membrane, it is probable that it plays a role in regulating the autophagic processes stimulated by nicotine. The results showed that downregulation of LAPTM4B expression in response to nicotine stimulation induced further upregulation of mRNA levels and protein levels of Col1, Col3, α-SMA and FN in CFs (Fig. 6A and B). The same results were shared in NRVMs, where nicotine-activated siLAPTM4B resulted in an increase in myocardial hypertrophic markers, ANP, BNP, and β-MHC mRNA levels (Fig. 6C). In contrast, the opposite result was observed after upregulation of LAPTM4B expression. Overexpression of LAPTM4B significantly attenuated nicotine-induced mRNA levels of Col1, Col3, α-SMA and FN (Fig. 6D), and the same results were observed at the protein level (Fig. 6E). AdLAPTM4B also decreased ANP, BNP and β-MHC mRNA levels in nicotine-stimulated NRVMs (Fig. 6F). Thus, downregulation of LAPTM4B exacerbates nicotine-induced activation of CFs and hypertrophy of NRVMs, which is similar to the effect of CDX1.

We then examined the effect of LAPTM4B in autophagy. It was found that downregulation of LAPTM4B in CFs further exacerbated nicotine-induced accumulation of LC3II and the autophagy substrate p62 (Fig. 7A). In contrast, upregulation of LAPTM4B alleviated nicotine-induced p62 accumulation, while LC3II expression remained unchanged (Fig. 7B). As illustrated in Figure S4G and 4 H, the same outcome was observed in NRVMs. The aforementioned data indicated that overexpression of LAPTM4B mitigated the nicotine-induced blockage of the autophagic process by promoting autophagy, whereas silencing LAPTM4B further impeded the autophagic flux and exacerbated CFs activation and cardiomyocyte hypertrophy.

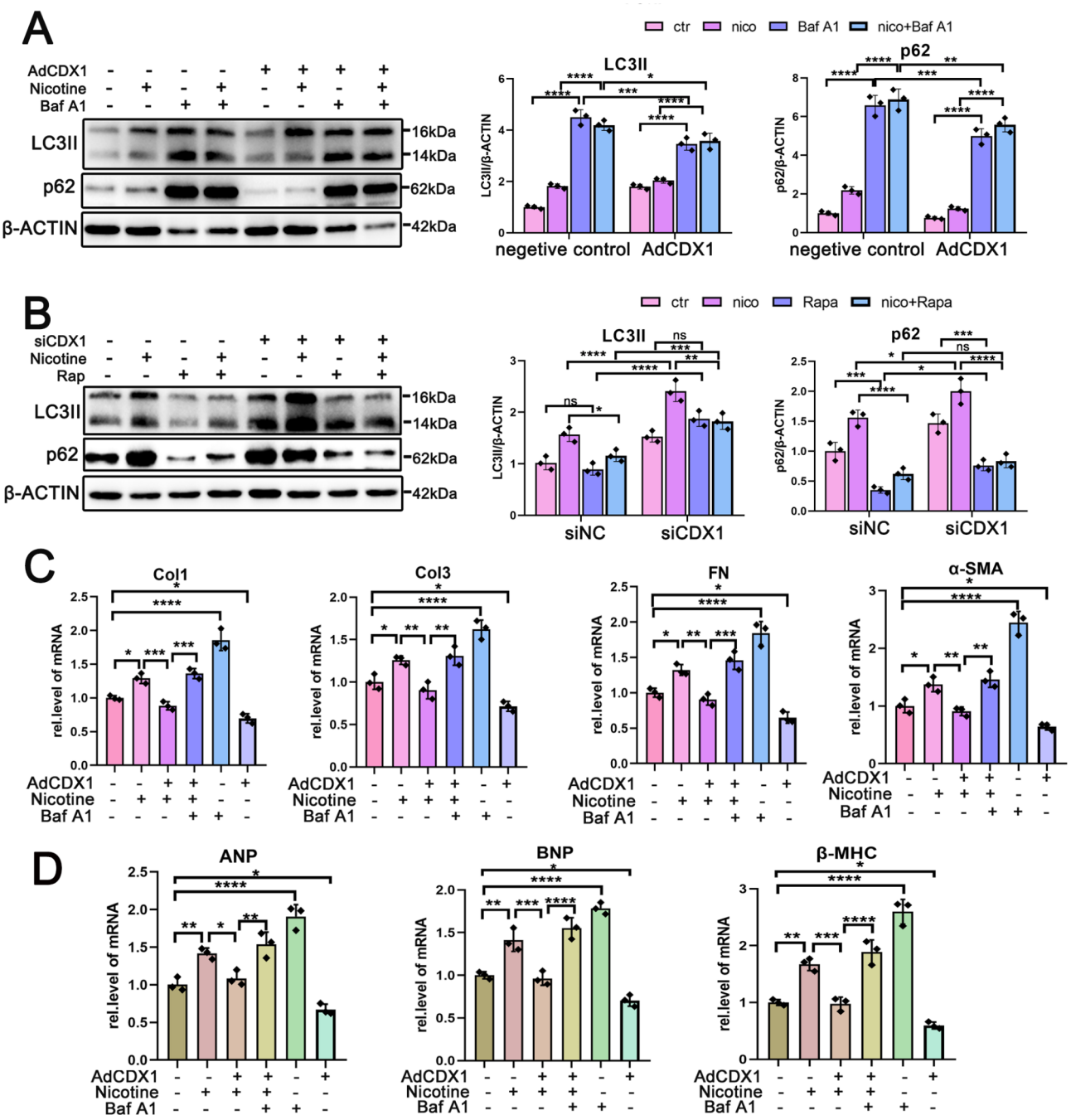

Fig. 4. Up-regulation of CDX1 alleviates autophagic flux blockade and down-regulation of CDX1 exacerbates autophagic flux blockade. WB detection of LC3II and p62 expression in CFs after AdCDX1 stimulation by Baf A1 and nicotine alone or in combination (**A**). WB detection of LC3II and p62 expression in CFs after siCDX1 stimulation by Rapa and nicotine alone or in combination (**B**). Results are given as mean ± SD, P value was determined by two-way AVONA with Bonferroni test, **** $p < 0.0001$; *** $p < 0.001$; ** $p < 0.01$; * $p < 0.05$, $n = 3$. Under nicotine and Baf A1 (100 nM) stimulation alone or in combination, qPCR was performed to detect mRNA expression of Col1, Col3, α-SMA and FN in CFs after CDX1 overexpression (**C**) and mRNA expression of ANP, BNP, β-MHC in NRVMs (**D**). Results are given as mean ± SD, P value was determined by one-way AVONA with Bonferroni test, **** $p < 0.0001$; *** $p < 0.001$; ** $p < 0.01$; * $p < 0.05$, $n = 3$.

CDX1 affects cardiomyocyte hypertrophy and cardiac fibroblast activation by regulating LAPTM4B-mediated autophagy

To further investigate the relationship between CDX1 and LAPTM4B in the regulation of autophagy and the mechanism of cardioprotective effects, we applied AdCDX1 and siLAPTM4B to co-transfect CFs and NRVMs. The results demonstrated that AdCDX1 alleviated nicotine-induced activation of CFs and cardiomyocyte

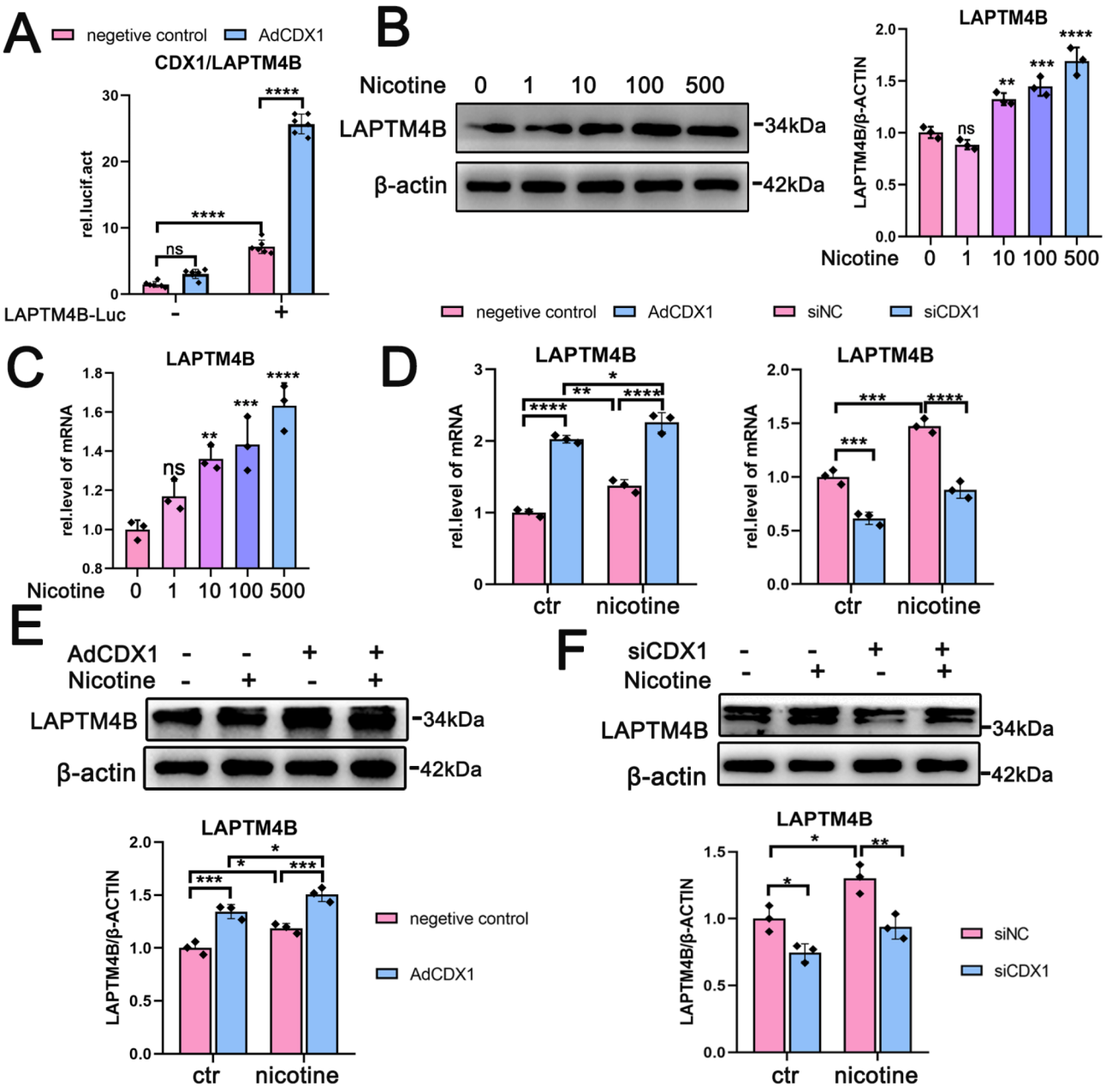

Fig. 5. LAPTM4B is upregulated in response to nicotine stimulation and CDX1 regulates LAPTM4B transcription. A dual luciferase reporter gene assay was used to analyse the relationship between the CDX1 transcription factor and the LAPTM4B promoter (**A**). Results are given as mean ± SD, P value was determined by one-way AVONA with Bonferroni test, **** $p < 0.0001$; *** $p < 0.001$; ** $p < 0.01$; * $p < 0.05$, $n = 6$. After nicotine stimulation of CFs, protein expression of LAPTM4B was detected by WB (**B**). qPCR was performed to detect mRNA expression of LAPTM4B (**C**). Results are given as mean ± SD, P value was determined by one-way AVONA with Bonferroni test, **** $p < 0.0001$; *** $p < 0.001$; ** $p < 0.01$; * $p < 0.05$, $n = 3$. After up- or down-regulation of CDX1 expression, mRNA expression of LAPTM4B was detected by qPCR in CFs with or without nicotine (**D**). After up- or down-regulation of CDX1 expression, protein expression of LAPTM4B was detected by WB (**E**–**F**). Results are given as mean ± SD, P value was determined by two-way AVONA with Bonferroni test, **** $p < 0.0001$; *** $p < 0.001$; ** $p < 0.01$; * $p < 0.05$, $n = 3$.

hypertrophy under nicotine stimulation. Compared to the AdCDX1 group, the mRNA levels of Col1, Col3, α-SMA, FN (Fig. 7C) and ANP, BNP, β-MHC (Fig. 7D) were elevated in the AdCDX1 + siLAPTM4B group, indicating that the downregulation of LAPTM4B counteracted the protective effect caused by the upregulation of CDX1.

In response to nicotine, AdCDX1 was observed to alleviate the accumulation of LC3II and p62. However, LC3II levels were found to increase further following AdCDX1 + siLAPTM4B treatment, while p62 also demonstrated

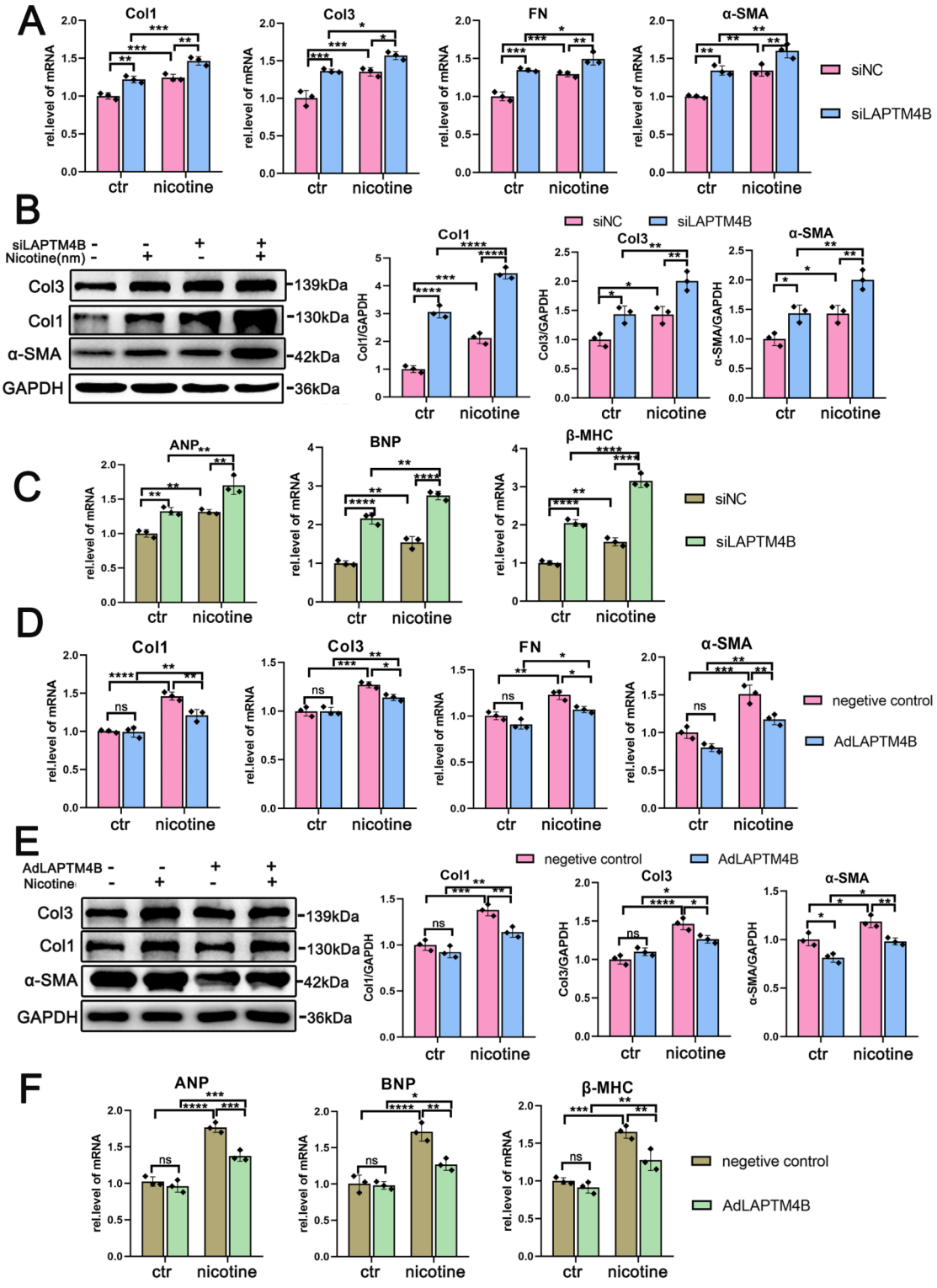

Fig. 6. Down-regulation of LAPTM4B promoted nicotine-induced activation of CFs and cardiomyocyte hypertrophy, whereas up-regulation of LAPTM4B had the opposite effect. qPCR was used to detect the mRNA expression of myocardial fibrosis markers Col1, Col3, α-SMA, FN in CFs when LAPTM4B was downregulated (**A**) and the mRNA expression of cardiac hypertrophy markers ANP, BNP and β-MHC in NRVMs (**C**). WB detected the expression of Col1, Col3, α-SMA after siLAPTM4B (**B**). Application of qPCR to detect the expression of Col1, Col3, α-SMA, FN in CFs (**D**) and the expression of ANP, BNP and β-MHC in NRVMs when LAPTM4B was overexpressed (**F**). WB was used to assess the protein expression levels of Col1, Col3, andα-SMA after AdLAPTM4B (**E**). Results are given as mean ± SD, P value was determined by two-way AVONA with Bonferroni test, **** $p < 0.0001$; *** $p < 0.001$; ** $p < 0.01$; * $p < 0.05$, $n = 3$.

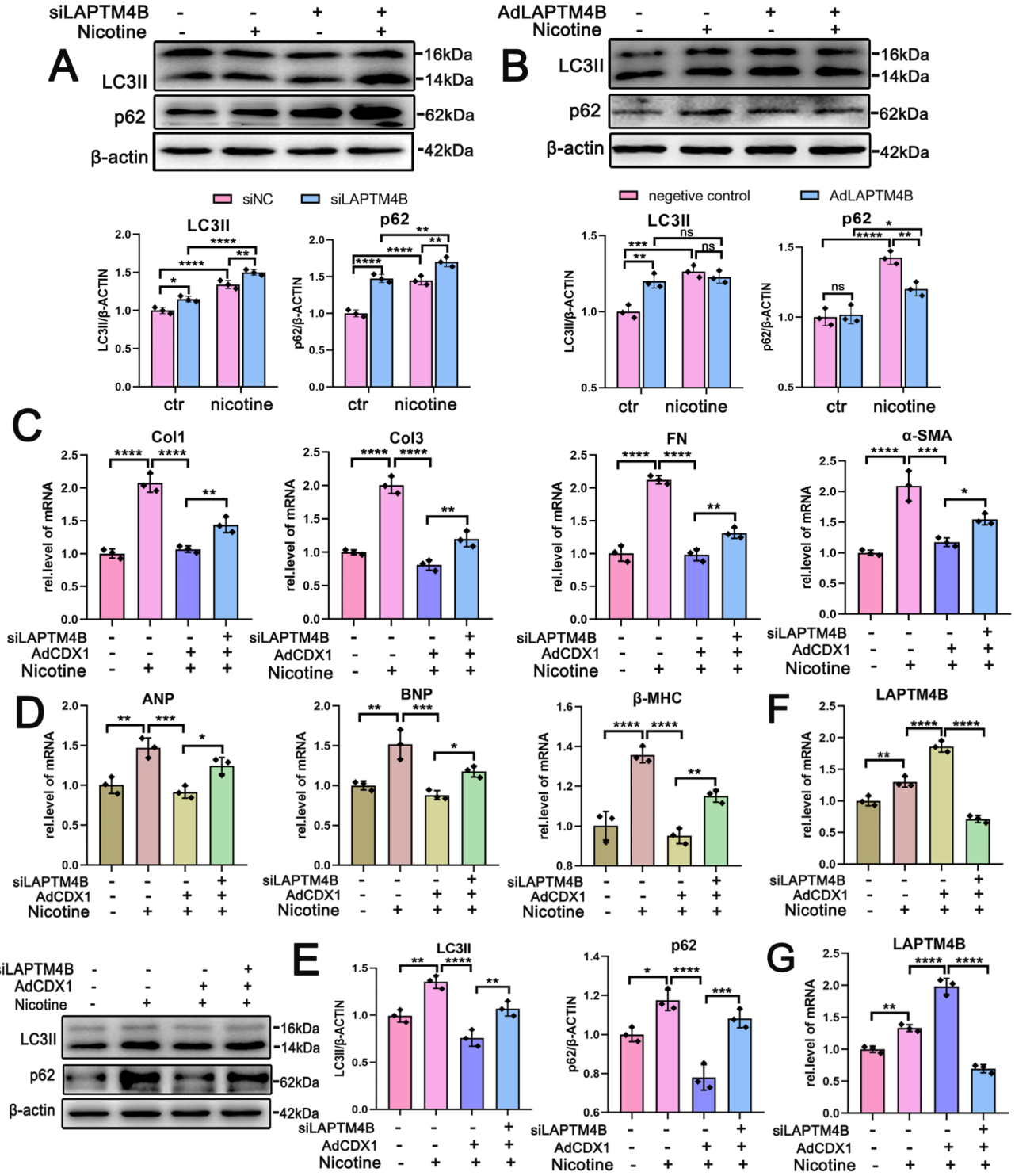

Fig. 7. CDX1 blocks autophagic flux and induces CFs activation and cardiomyocyte hypertrophy by regulating LAPTM4B downregulation. WB detection of LC3II and p62 expression levels in LAPTM4B knockdown (**A**) or overexpression (**B**) in CFs. Results are given as mean ± SD, P value was determined by two-way AVONA with Bonferroni test, **** $p < 0.0001$; *** $p < 0.001$; ** $p < 0.01$; * $p < 0.05$, $n = 3$. After co-transfection of CFs and NRVMs by application of AdCDX1 and siLAPTM4B, qPCR was applied to detect the expression of Col1, Col3, α-SMA, FN (**C**) and ANP, BNP, β-MHC (**D**). WB was used to detect the expression of LC3II and p62 in CFs co-transfected with AdCDX1 and siLAPTM4B (**E**). qPCR was used to detect the mRNA expression of LAPTM4B in CFs (**G**) and NRVMs (**F**) co-transfected with AdCDX1 and siLAPTM4B. Results are given as mean ± SD, P value was determined by one-way AVONA with Bonferroni test, **** $p < 0.0001$; *** $p < 0.001$; ** $p < 0.01$; * $p < 0.05$, $n = 3$.

further accumulation. This indicated that the downregulation of LAPTM4B in response to nicotine stimulation resulted in the elimination of the restoration of autophagic flux brought about by overexpression of CDX1, and the re-emergence of the blockage of the autophagic process (Fig. 7E). The same results were observed in NRVMs as well (Figure S4I). As demonstrated in Fig. 7F-G, siRNA-mediated knockdown of LAPTM4B decreased its mRNA levels to about 70% compared to the control group. These results indicated that CDX1 upregulation can safeguard the myocardium by regulating autophagy and restoring the impaired autophagic flux. This protective mechanism can be negated by LAPTM4B downregulation. Taken together, in the context of nicotine-induced cardiomyocyte hypertrophy and cardiac fibroblast activation, CDX1 exerted a similar action to LAPTM4B in the regulation of autophagy, and CDX1 positively regulates LAPTM4B.

CDX1/LAPTM4B affects autophagy flux through the mTORC1 signaling pathway

Following our findings on the role of CDX1 and LAPTM4B in nicotine-induced myocardial remodeling, we proceeded to investigate the signaling pathways involved in the regulation of autophagic flux by CDX1 and LAPTM4B. One key protein in this pathway is mTOR, which is a target of rapamycin. mTOR can form the mTORC1 complex, and its activation is closely linked to the blockade of autophagic flux. However, it remains unclear whether CDX1/LAPTM4B regulates autophagy by modulating the mTORC1 signaling pathway. As illustrated in Fig. 8A, the phosphorylation levels of mTOR, 4EBP1 and p70s6K were markedly elevated in response to nicotine stimulation. However, overexpression of CDX1 was observed to effectively reverse the nicotine-induced activation of mTOR, 4EBP1 and p70s6K. Conversely, the downregulation of CDX1 expression resulted in the overactivation of the phosphorylation levels of mTOR, 4EBP1 and p70s6K, which were further activated by nicotine, thereby blocking the process of autophagy (Fig. 8B). Similarly, the up-regulation of LAPTM4B in response to nicotine stimulation resulted in the alleviation of the activation of the mTORC1 complex caused by nicotine damage (Fig. 8C). Following the silencing of LAPTM4B, a comparable effect was observed on the mTOR signaling pathway to that observed with siCDX1 (Fig. 8D). It is therefore evident that CDX1/LAPTM4B may be involved in the regulation of autophagy and may reverse the nicotine-induced blockade of autophagic flux, thereby protecting the cardiomyocytes by modulating the mTORC1 signaling pathway.

Discussion

In the present study, we demonstrated for the first time that CDX1 restores the nicotine-induced blockade of autophagic flux and reverses the nicotine-induced activation of CFs and hypertrophy of NRVMs. This action protects cardiomyocytes function by promoting the transcription of LAPTM4B and thus inhibiting the mammalian target of rapamycin (mTOR) signaling pathway. First, the present study demonstrated that nicotine induces CFs activation and cardiomyocyte hypertrophy by impairing autophagic flux. Research predicts that heart failure will remain one of the most important diseases affecting human health by 2030[34,38], and improving myocardial remodeling has become an important part of the prevention and treatment of heart failure. The search for new targets to reverse myocardial remodeling has become the focus of current research. Studies have shown that nicotine is involved in the development of many cardiovascular diseases such as heart failure, hypertension and atherosclerosis[39–41]. In contrast, the study on the pathophysiological process of nicotine-regulated autophagy is not yet comprehensive. As the main alkaloid in cigarette smoke, nicotine is rapidly absorbed into the circulatory system, with blood levels reaching 40–100 ng/mL (about 240–610 nmol/L) after smoking one cigarette[42]. Among habitual smokers, the average plasma nicotine concentration usually ranges from 10 to 40 ng/mL, and tissue levels in the brain and heart can exceed plasma levels by 2–3 times[41]. In our experimental protocol using neonatal rat ventricular myocytes (NRVMs), we utilized a nicotine concentration of 100 μmol/L, which has been pharmacologically validated in previous investigations[16,43]. Interestingly, in cardiac fibroblasts (CFs), we demonstrated that cellular activation could be induced at substantially lower nicotine concentrations. Therefore, based on empirical evidence from prior studies[44], we established an optimal stimulation concentration of 500 nmol/L for CFs experiments.In this process, we observed a notable increase in CDX1 levels in response to nicotine stimulation, whereas CDX1 is minimally expressed in the heart in the normal state. The CDX1 gene encodes a transcriptional regulator that is highly expressed in the early stages of the embryo and plays a crucial role in heart development[18]. However, there are no reports on the effects of CDX1 on heart disease. The present study confirms that decreased CDX1 exacerbates nicotine-induced CFs activation and cardiomyocyte hypertrophy. Elevated CDX1 expression antagonizes nicotine-induced damage to cardiomyocytes and alleviates the development of CFs activation and cardiomyocyte hypertrophy. CDX1 is activated and upregulated during stress and can play a transcriptional regulatory role to protect the damaged myocardium. Abnormalities in autophagy have been shown to play a key role in myocardial remodeling. In tumor cells, CDX1 can inhibit apoptosis in colon cancer cells by activating autophagy[20]. In cardiomyocytes, whether CDX1 affects the heart by regulating autophagy has not been reported. Our study found that autophagic vesicles accumulated and autophagic flux was blocked after CDX1 reduction and aggravated nicotine-induced autophagic flux blockade. The classical autophagy activator Rapa mitigated these effects. The opposite trend was observed after increased CDX1 expression. However, BafA1 abrogated the protective effect on cardiomyocytes after CDX1 overexpression. Thus, CDX1 is involved in the process of influencing CFs activation and cardiomyocyte hypertrophy by regulating autophagic flux and exerts a protective effect on CFs and cardiomyocytes by alleviating the blockage of autophagic processes.

LAPTM4B is a 4-fold transmembrane structure on the lysosome that has been shown to be highly expressed in myocardium[23] and upregulated in response to nicotine stimulation[22,28]. By site prediction, we hypothesised that the CDX1 transcription factor and LAPTM4B might be correlated, but the specific relationship has not been reported in related studies. In this study, we found that the CDX1 transcription factor promotes LAPTM4B transcription.CDX1 transcription factor may specifically bind to the promoter of LAPTM4B and positively regulate the expression of LAPTM4B at the transcriptional level. And LAPTM4B was similarly upregulated in response to nicotine stimulation. Recent studies have reported that LAPTM4B can alleviate autophagic flux

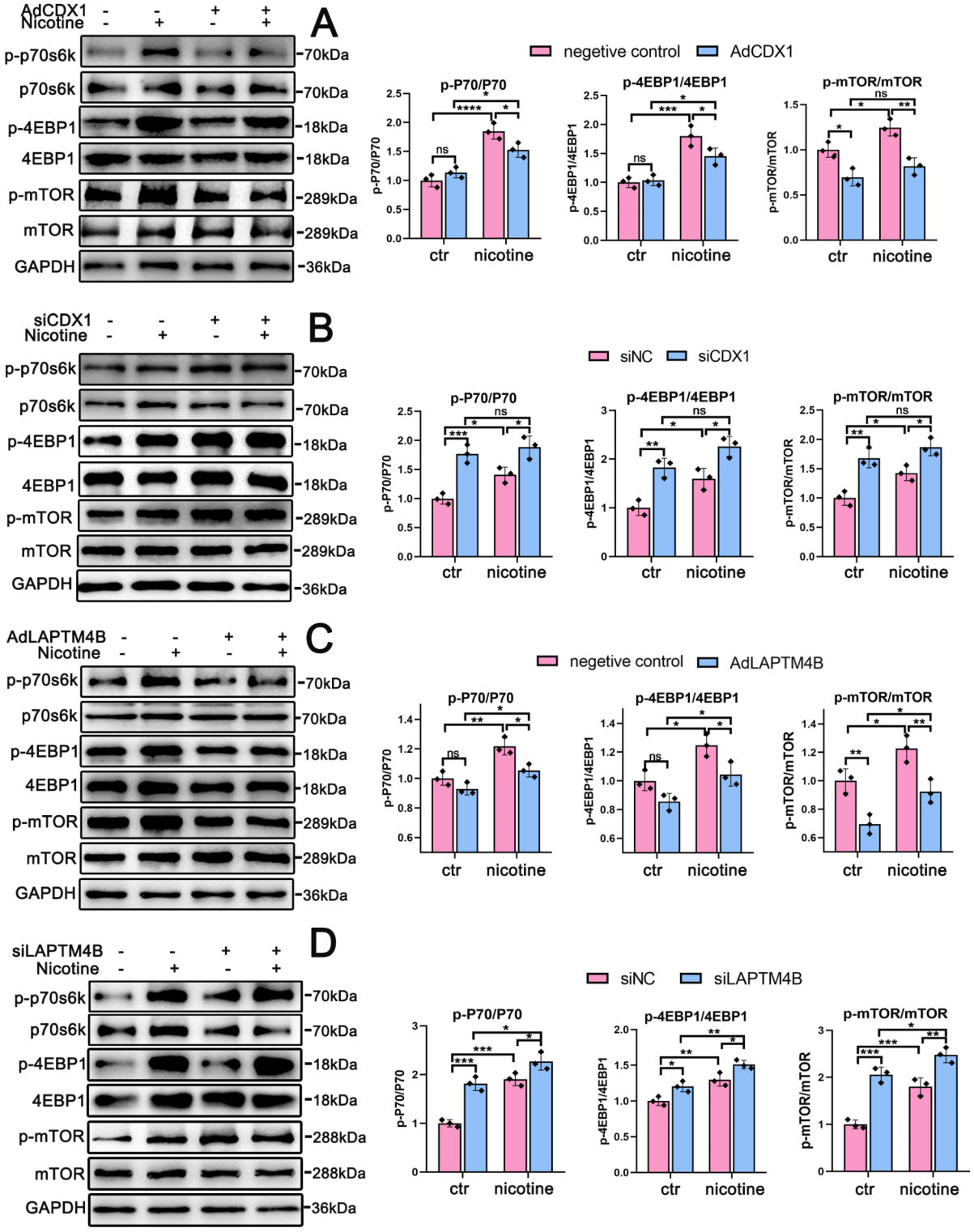

Fig. 8. CDX1/LAPTM4B affects autophagy levels through the mTORC1 signalling pathway. With or without nicotine stimulation, Westernblot was applied to detect the phosphorylation level of p70s6k,4EBP1,mTOR after overexpression of CDX1 (**A**) or inhibition of CDX1 expression (**B**). expression of LAPTM4B was up-regulated (**C**) or down-regulated (**D**), and Westernblot was applied to detect the p70s6k,4EBP1,mTOR phosphorylation levels. Results are given as mean ± SD, P value was determined by two-way AVONA with Bonferroni test, **** $p < 0.0001$; *** $p < 0.001$; ** $p < 0.01$; * $p < 0.05$, $n = 3$.

blockade by enhancing autophagic lysosomes and promoting autophagosomal clearance during myocardial I/R injury, thereby reducing myocardial injury[26]. The role of LAPTM4B in nicotine-induced myocardial injury remains unknown. The results of the present study show that downregulation of LAPTM4B exacerbates the activation of CFs and hypertrophy of myocardial cell in response to nicotine, whereas an increase in LAPTM4B reverses this detrimental effect of nicotine. Thus, our results show that LAPTM4B is also involved in the process of CFs activation and cardiomyocyte hypertrophy by regulating autophagy: autophagic vesicles accumulate and autophagic flux is blocked by a decrease in LAPTM4B, whereas an increase in LAPTM4B restores nicotine-blocked autophagic flux and protects the myocardium. Importantly, the protective effect on cardiomyocytes that occurs with upregulation of CDX1 can be abolished by downregulation of LAPTM4B, and the autophagic flux that is restored after CDX1 overexpression is blocked again by reduced expression of LAPTM4B. It is therefore clear that CDX1 promotes the restoration of autophagic flux under the influence of nicotine by positively regulating the transcription of LAPTM4B, thereby exerting a protective effect on cardiomyocytes.

mTORC1 is the classical pathway of autophagy and studies have shown that inhibiting the activation of mTORC1 can improve the progression of heart failure by promoting autophagy and inhibiting apoptosis[45]. In the heart, LAPTM4B can reduce cardiac injury in ischaemia/reperfusion by inhibiting the activation of mTORC1[26]. During in the embryonic stage, CDX1 also regulates stem cell differentiation through the mTOR pathway[19]. And whether CDX1/LAPTM4B regulates the onset of CFs activation and myocardial cell hypertrophy through the mTORC1 signaling pathway during nicotine-induced myocardial injury is unknown. Our study found that during nicotine-induced CFs activation and myocardial cell hypertrophy, nicotine could block the normal autophagic process by promoting the activation of mTORC1, which induced the activation of CFs and the development of cardiomyocyte hypertrophy. Rapa alleviates nicotine-induced CFs activation and NRVMs hypertrophy by activating autophagy. However, the transcription factor CDX1 and its downstream target protein, LAPTM4B, can reverse this effect and slow down the development of CFs activation and myocardial cell hypertrophy by inhibiting the activation of mTORC1. This function is broadly similar to their role in tumour cells, where high levels of both CDX1 and LAPTM4B inhibit tumor cell proliferation and are associated with a better prognosis[46,47]. It is worth noting that the up-regulation of CDX1 and LAPTM4B in response to nicotine stimulation was small and this level may not be sufficient to completely antagonize the effects of nicotine, but they remain important as a link in the self-protection mechanism of cardiomyocytes. In our study, we observed that although overexpression of CDX1 can mitigate nicotine-induced cardiomyocyte injury in both CFs and NRVMs, cardiomyocytes still exhibit detrimental responses to nicotine stimulation. This suggests that, in addition to the CDX1/mTOR signaling pathway, nicotine stimulation may activate multiple other signaling pathways independent of CDX1, which are involved in the processes of cardiomyocyte hypertrophy and fibroblast activation. Further investigation is required to elucidate these additional mechanisms. As the present study was only carried out at the cellular level and has not been validated at the animal level, there are some limitations that need to be confirmed by more and deeper studies in the future.

In conclusion, the results of the present study suggest that the transcription factor CDX1 and its downstream target protein LAPTM4B alleviate nicotine-induced autophagic flux impairment by inhibiting the activation of the mTOR pathway, thereby reversing cardiomyocyte hypertrophy and fibroblast activation and exerting cardioprotective functions. This provides new targets and ideas for investigating the mechanism of myocardial remodeling.

Data availability

The data supporting the findings of this study are included in this published article. Raw data generated and/or analysed during the current study are available from the corresponding author, upon reasonable request.

Received: 7 December 2024; Accepted: 12 March 2025
Published online: 22 March 2025

References

1. de Couto, G., Ouzounian, M. & Liu, P. P. Early detection of myocardial dysfunction and heart failure. *Nat. Reviews Cardiol.* **7**, 334–344. https://doi.org/10.1038/nrcardio.2010.51 (2010).
2. Dupree, C. S. Primary prevention of heart failure: An update. *Curr. Opin. Cardiol.* **25**, 478–483. https://doi.org/10.1097/HCO.0b013e32833cd550 (2010).
3. Li, N. et al. Nicotine induces cardiomyocyte hypertrophy through TRPC3-Mediated Ca(2+)/NFAT signalling pathway. *Can. J. Cardiol.* **32**, 1260e1. https://doi.org/10.1016/j.cjca.2015.12.015 (2016).
4. Reis Junior, D. et al. Association of exercise training with tobacco smoking prevents fibrosis but has adverse impact on myocardial mechanics. *Nicotine Tob. Research: Official J. Soc. Res. Nicotine Tob.* **18**, 2268–2272. https://doi.org/10.1093/ntr/ntw180 (2016).
5. Yu, G. et al. The effect of cigarette smoking on the oral and nasal microbiota. *Microbiome* **5**, 3. https://doi.org/10.1186/s40168-016-0226-6 (2017).
6. Aredo, J. V. et al. Tobacco smoking and risk of second primary lung cancer. *J. Thorac. Oncol.: Off. Publ. Int. Assoc. Study Lung Cancer* **16**, 968–979. https://doi.org/10.1016/j.jtho.2021.02.024 (2021).
7. Wang, S. Y. et al. Cilostazol alleviate nicotine induced cardiomyocytes hypertrophy through modulation of autophagy by CTSB/ROS/p38MAPK/JNK feedback loop. *Int. J. Biol. Sci.* **16**, 2001–2013. https://doi.org/10.7150/ijbs.43825 (2020).
8. Zhang, H. et al. Necroptosis mediated by impaired autophagy flux contributes to adverse ventricular remodeling after myocardial infarction. *Biochem. Pharmacol.* **175**, 113915. https://doi.org/10.1016/j.bcp.2020.113915 (2020).
9. Han, X., Zhang, Y. L., Lin, Q. Y., Li, H. H. & Guo, S. B. ATGL deficiency aggravates pressure overload-triggered myocardial hypertrophic remodeling associated with the proteasome-PTEN-mTOR-autophagy pathway. *Cell Biol. Toxicol.* **39**, 2113–2131. https://doi.org/10.1007/s10565-022-09699-0 (2023).
10. Deng, H. F. et al. Nicorandil alleviates cardiac remodeling and dysfunction post -infarction by up-regulating the nucleolin/autophagy axis. *Cell. Signal.* **92**, 110272. https://doi.org/10.1016/j.cellsig.2022.110272 (2022).
11. Yamamoto, H., Zhang, S. & Mizushima, N. Autophagy genes in biology and disease. *Nat. Rev. Genet.* **24**, 382–400. https://doi.org/10.1038/s41576-022-00562-w (2023).

12. Lin, L. et al. Pyroptosis, and ferroptosis: new regulatory mechanisms for atherosclerosis. *Front. Cell. Dev. Biol.* **9**, 809955. https://doi.org/10.3389/fcell.2021.809955 (2021).
13. Bhuiyan, M. S. et al. Enhanced autophagy ameliorates cardiac proteinopathy. *J. Clin. Investig.* **123**, 5284–5297. https://doi.org/10.1172/jci70877 (2013).
14. Lin, L. et al. Mas receptor mediates cardioprotection of angiotensin-(1–7) against angiotensin II-induced cardiomyocyte autophagy and cardiac remodelling through Inhibition of oxidative stress. *J. Cell. Mol. Med.* **20**, 48–57. https://doi.org/10.1111/jcmm.12687 (2016).
15. Xiao, Y. et al. TAX1BP1 overexpression attenuates cardiac dysfunction and remodeling in STZ-induced diabetic cardiomyopathy in mice by regulating autophagy. *Biochim. Et Biophys. Acta Mol. Basis Dis.* **1864**, 1728–1743. https://doi.org/10.1016/j.bbadis.2018.02.012 (2018).
16. Kanamori, H. et al. The role of autophagy emerging in postinfarction cardiac remodelling. *Cardiovascular. Res.* **91**, 330–339. https://doi.org/10.1093/cvr/cvr073 (2011).
17. Zheng, H. et al. Low CDX1 expression predicts a poor prognosis for hepatocellular carcinoma patients after hepatectomy. *Surg. Oncol.* **25**, 171–177. https://doi.org/10.1016/j.suronc.2016.05.026 (2016).
18. Plateroti, M., Freund, J. N., Leberquier, C. & Kedinger, M. Mesenchyme-mediated effects of retinoic acid during rat intestinal development. *J. Cell Sci.* **110**(Pt 10), 1227–1238. https://doi.org/10.1242/jcs.110.10.1227 (1997).
19. Lei, D., Sun, H. & Zhang, B. MiR-24 promotes cell growth in human glioma by CDX1/PI3K/Akt signaling pathway. *Cancer Biother. Radiopharm.* **36**, 588–599. https://doi.org/10.1089/cbr.2020.3711 (2021).
20. Wu, S., Wang, X., Chen, J. & Chen, Y. Autophagy of cancer stem cells is involved with chemoresistance of colon cancer cells. *Biochem. Biophys. Res. Commun.* **434**, 898–903. https://doi.org/10.1016/j.bbrc.2013.04.053 (2013).
21. Parenti, G., Andria, G. & Ballabio, A. Lysosomal storage diseases: From pathophysiology to therapy. *Annu. Rev. Med.* **66**, 471–486. https://doi.org/10.1146/annurev-med-122313-085916 (2015).
22. Meng, Y. et al. LAPTM4B: An oncogene in various solid tumors and its functions. *Oncogene* **35**, 6359–6365. https://doi.org/10.1038/onc.2016.189 (2016).
23. Shao, G. Z. et al. Molecular cloning and characterization of LAPTM4B, a novel gene upregulated in hepatocellular carcinoma. *Oncogene* **22**, 5060–5069. https://doi.org/10.1038/sj.onc.1206832 (2003).
24. Li, Y., Iglehart, J. D., Richardson, A. L. & Wang, Z. C. The amplified cancer gene LAPTM4B promotes tumor growth and tolerance to stress through the induction of autophagy. *Autophagy* **8**, 273–274. https://doi.org/10.4161/auto.8.2.18941 (2012).
25. Tan, X., Thapa, N., Sun, Y. & Anderson, R. A. A kinase-independent role for EGF receptor in autophagy initiation. *Cell* **160**, 145–160. https://doi.org/10.1016/j.cell.2014.12.006 (2015).
26. Gu, S. et al. Downregulation of LAPTM4B contributes to the impairment of the autophagic flux via unopposed activation of mTORC1 signaling during myocardial ischemia/reperfusion injury. *Circul. Res.* **127**, e148–e165. https://doi.org/10.1161/circresaha.119.316388 (2020).
27. Paulo, J. A. & Gygi, S. P. Nicotine-induced protein expression profiling reveals mutually altered proteins across four human cell lines. *Proteomics* **17** https://doi.org/10.1002/pmic.201600319 (2017).
28. Maki, Y. et al. LAPTM4B is associated with poor prognosis in NSCLC and promotes the NRF2-mediated stress response pathway in lung cancer cells. *Sci. Rep.* **5**, 13846. https://doi.org/10.1038/srep13846 (2015).
29. Liu, G. Y. & Sabatini, D. M. mTOR at the nexus of nutrition, growth, ageing and disease. *Nat. Rev. Mol. Cell Biol.* **21**, 183–203. https://doi.org/10.1038/s41580-019-0199-y (2020).
30. Savini, M., Zhao, Q., Wang, M. C. & Lysosomes Signaling hubs for metabolic sensing and longevity. *Trends Cell Biol.* **29**, 876–887. https://doi.org/10.1016/j.tcb.2019.08.008 (2019).
31. Sciarretta, S., Forte, M., Frati, G. & Sadoshima, J. New insights into the role of mTOR signaling in the cardiovascular system. *Circul. Res.* **122**, 489–505. https://doi.org/10.1161/circresaha.117.311147 (2018).
32. Buss, S. J. et al. Beneficial effects of mammalian target of rapamycin inhibition on left ventricular remodeling after myocardial infarction. *J. Am. Coll. Cardiol.* **54**, 2435–2446. https://doi.org/10.1016/j.jacc.2009.08.031 (2009).
33. Li, Q. et al. Overexpression of microRNA-99a attenuates heart remodelling and improves cardiac performance after myocardial infarction. *J. Cell. Mol. Med.* **18**, 919–928. https://doi.org/10.1111/jcmm.12242 (2014).
34. Yang, M., Lu, Y., Piao, W. & Jin, H. The translational regulation in mTOR pathway. *Biomolecules* **12** https://doi.org/10.3390/biom12060802 (2022).
35. Li, Y. et al. Sphingosylphosphorylcholine alleviates hypoxia-caused apoptosis in cardiac myofibroblasts via CaM/p38/STAT3 pathway. *Apoptosis: Int. J. Program. Cell. Death.* **25**, 853–863. https://doi.org/10.1007/s10495-020-01639-9 (2020).
36. Li, Y. et al. Adiponectin upregulates MiR-133a in cardiac hypertrophy through AMPK activation and reduced ERK1/2 phosphorylation. *PloS One.* **11**, e0148482. https://doi.org/10.1371/journal.pone.0148482 (2016).
37. Li, Y. et al. Novel Ferrocenyl derivatives exert anti-cancer effect in human lung cancer cells in vitro via inducing G1-phase arrest and senescence. *Acta Pharmacol. Sin.* **34**, 960–968. https://doi.org/10.1038/aps.2013.19 (2013).
38. Mathers, C. D. & Loncar, D. Projections of global mortality and burden of disease from 2002 to 2030. *PLoS Med.* **3**, e442. https://doi.org/10.1371/journal.pmed.0030442 (2006).
39. Lee, H. & Son, Y. J. Influence of smoking status on risk of incident heart failure: A systematic review and Meta-Analysis of prospective cohort studies. *Int. J. Environ. Res. Public Health* **16** https://doi.org/10.3390/ijerph16152697 (2019).
40. He, X. et al. Prenatal nicotine exposure induces HPA axis-hypersensitivity in offspring rats via the intrauterine programming of up-regulation of hippocampal GAD67. *Arch. Toxicol.* **91**, 3927–3943. https://doi.org/10.1007/s00204-017-1996-8 (2017).
41. Benowitz, N. L. & Burbank, A. D. Cardiovascular toxicity of nicotine: Implications for electronic cigarette use. *Trends Cardiovasc. Med.* **26**, 515–523. https://doi.org/10.1016/j.tcm.2016.03.001 (2016).
42. Vang, A. et al. Effect of A7 nicotinic acetylcholine receptor activation on cardiac fibroblasts: a mechanism underlying RV fibrosis associated with cigarette smoke exposure. *Am. J. Physiol. Lung Cell. Mol. Physiol.* **312**, L748–l759. https://doi.org/10.1152/ajplung.00393.2016 (2017).
43. Aberle, N. S., Privratsky, J. R., Burd, L., Ren, J. & nd, and Combined acetaldehyde and nicotine exposure depresses cardiac contraction in ventricular myocytes: prevention by folic acid. *Neurotoxicol. Teratol.* **25**, 731–736. https://doi.org/10.1016/j.ntt.2003.07.008 (2003).
44. Wu, H. H. et al. LDHA contributes to nicotine induced cardiac fibrosis through autophagy flux impairment. *Int. Immunopharmacol.* **136**, 112338. https://doi.org/10.1016/j.intimp.2024.112338 (2024).
45. Gao, G. et al. Rapamycin regulates the balance between cardiomyocyte apoptosis and autophagy in chronic heart failure by inhibiting mTOR signaling. *Int. J. Mol. Med.* **45**, 195–209. https://doi.org/10.3892/ijmm.2019.4407 (2020).
46. Ji, H. et al. Two circPPFIA1s negatively regulate liver metastasis of colon cancer via miR-155-5p/CDX1 and HuR/RAB36. *Mol. Cancer* **21**, 197. https://doi.org/10.1186/s12943-022-01667-w (2022).
47. Luk, I. Y. et al. Epithelial de-differentiation triggered by co-ordinate epigenetic inactivation of the EHF and CDX1 transcription factors drives colorectal cancer progression. *Cell Death Differ.* **29**, 2288–2302. https://doi.org/10.1038/s41418-022-01016-w (2022).

Author contributions

Y.Y.L., G.H.S, and Y.L. conceptualized this idea. Y.Y.L., F.L.M., S.Y.Z., and J.M.D. performed the experiments. W.J.L.,Q.Y.L., L.W., M.M.Z., Q.Y.Z. and Y.J. analyzed and interpreted the data. Y.Y.L., G.H.S., and Y.L.. wrote the

paper. All authors helped with the revision of the draft.

Funding
This work was supported by the National Natural Science Foundation of China (81700217), Shandong Provincial Natural Science Foundation (ZR2023MH288, ZR2021MH019, and ZR2016HB57), China Postdoctoral Science Foundation (2019M662370), Shandong Province Postdoctoral Innovation Project (202003046), Jinan Medical Science and Technology Innovation Project (202225025) and National Major Scientific and Technological Special Project for "Significant New Drugs Development" of China (2020ZX09201025).

Declarations

Competing interests
The authors declare no competing interests.

Ethical approval
The experimental procedures carried out in the present study were approved by the Animal Ethics Committee of Jinan Central Hospital (approval no. JNCHIACUC2024-42). All procedure were performed in accordance with the ethical standards of the guidelines and ARRIVE guidelines.

Additional information
Supplementary Information The online version contains supplementary material available at https://doi.org/10.1038/s41598-025-94160-5.

Correspondence and requests for materials should be addressed to Y.L. or G.-h.S.

Reprints and permissions information is available at www.nature.com/reprints.

Publisher's note Springer Nature remains neutral with regard to jurisdictional claims in published maps and institutional affiliations.